

Hierarchically Structured Nanoporous Poly(Ionic Liquid) Membranes: Facile Preparation and Application in Fiber-Optic pH Sensing

Qiang Zhao,[†] Mingjie Yin,[‡] A. Ping Zhang,[‡] Simon Prescher,[†] Markus Antonietti,[†] and Jiayin Yuan^{*,†}

[†]Department of Colloid Chemistry, Max Planck Institute of Colloids and Interfaces, D-14424 Potsdam, Germany

[‡]Photonics Research Centre, Department of Electrical Engineering, The Hong Kong Polytechnic University, Kowloon, Hong Kong SAR, China

S Supporting Information

ABSTRACT: Nanoporous polyelectrolyte membranes with hierarchical and unique pore architectures can be readily made via electrostatic complexation between imidazolium-based poly(ionic liquid)s and poly(acrylic acid) in a variety of morphologies. Coating the membrane onto the surface of an optical fiber resulted in a device with high pH-sensing performance in terms of the response rate and the sensitivity, due to the charge and porous nature of the membrane layer.

Porous polymeric membranes are receiving increasing research interest in both academia and industry because such systems build up a multifunctional platform for fundamental research and many practical usages.¹ In this regard, porous polyelectrolyte membranes (PPMs) are particularly appealing because the additionally introduced charged character, along with their high mechanical and chemical stability, renders them versatile for device fabrication and attractive applications such as separation, controlled release, catalyst supports, biointerfacing, and sensors, just to name a few.² In industry, there are already two well-established methods for preparing porous membranes, namely, non-solvent-induced phase separation (NIPS) and thermally induced phase separation (TIPS).^{1g} However, the water solubility and ionic nature of common polyelectrolytes make them difficult to use in preparing PPMs by these two methods. The self-assembly and dewetting approaches,³ though widely adopted in research laboratories to obtain nanoporous films from block copolymers or their blends, are somehow inappropriate for preparing PPMs. Hence, in comparison with some relatively easy pathways to (sub)micrometer sized large pores, such as the freezing/drying method,⁴ constructing well-defined nanopores inside polyelectrolyte membranes has been a long-standing challenge. To date, this has been partially accomplished by solution post-treatment or template processing of multilayered polyelectrolyte complex coatings prepared via electrostatic layer-by-layer (LbL) assembly of specific building blocks under carefully designed conditions.^{4d,e,5} Even in these studies, freestanding PPMs were difficult to obtain.^{5g} Moreover, though conceptually simple and straightforward,⁶ the LbL approach is comparatively time- and labor-demanding and difficult to scale.

Here we demonstrate for the first time a facile and efficient template-free route to PPMs by exploiting electrostatic

complexation between a cationic poly(ionic liquid) or polymerized ionic liquid (PIL) and a polyanion. Notably, this approach simultaneously integrates the membrane formation and nanopore creation processes into a single and rather simple soaking procedure, affording a beneficial feature not available to any other membrane fabrication and polyelectrolyte complexation process.⁷ The as-prepared nanoporous membranes are structurally robust at processing pressures and stable under various environmental conditions, allowing their use not only in traditional freestanding or composite membrane applications but also as functional coatings compatible with practical devices. This was further exemplified here by the creation of a highly sensitive and rapidly responsive fiber-optic pH sensor.

Figure 1a illustrates the synthetic procedure leading to the hierarchically structured PPMs. The model cationic polyelectrolyte component was an imidazolium-based PIL, poly[1-cyanomethyl-3-vinylimidazolium bis(trifluoromethanesulfonyl)imide] (PCMVImTf₂N).⁸ The anionic counterpart was poly(acrylic acid) (PAA), a common weak polyelectrolyte. PCMVImTf₂N and PAA were fully dissolved in dimethylformamide (DMF) solvent in a 1:1 equivalent molar ratio based on monomer units. The formed homogeneous solution was then cast onto a glass plate and dried at 80 °C for 1 h (the film surfaces facing the air and the glass plate are called the top and bottom surfaces, respectively). In a second step, the film was immersed in a 0.2 wt % aqueous NH₃ solution (pH 10.8, 20 °C) or a 0.01 M aqueous NaOH solution for 2 h. This process led to charging of the acrylic acid moieties, restructuring of the film on the nanoscale level, and finally the formation of a stable nanopore structure within the film. Afterward, a yellowish, flexible, freestanding membrane with an overall size of up to tens of centimeters (Figure 1b) was readily obtained. It was tested in a 0.5 M aqueous NaCl solution over a pH range of 1–12 for 10 h, and no structural damage was detected. All of these speak to the high mechanical and chemical stability of this paperlike membrane. The robustness of the membrane was also confirmed by the stable water permeation observed in a continuous filtration test (3 bar pressure) for 96 h.

In reference experiments, membranes could not be obtained from the pristine PCMVImTf₂N and PAA polymer solutions because of their poor mechanical interconnection or by soaking the PVImTf₂N/PAA physical blend in neutral water without NH₃. This clearly indicates that neutralization by NH₃

Received: February 27, 2013

Published: April 1, 2013

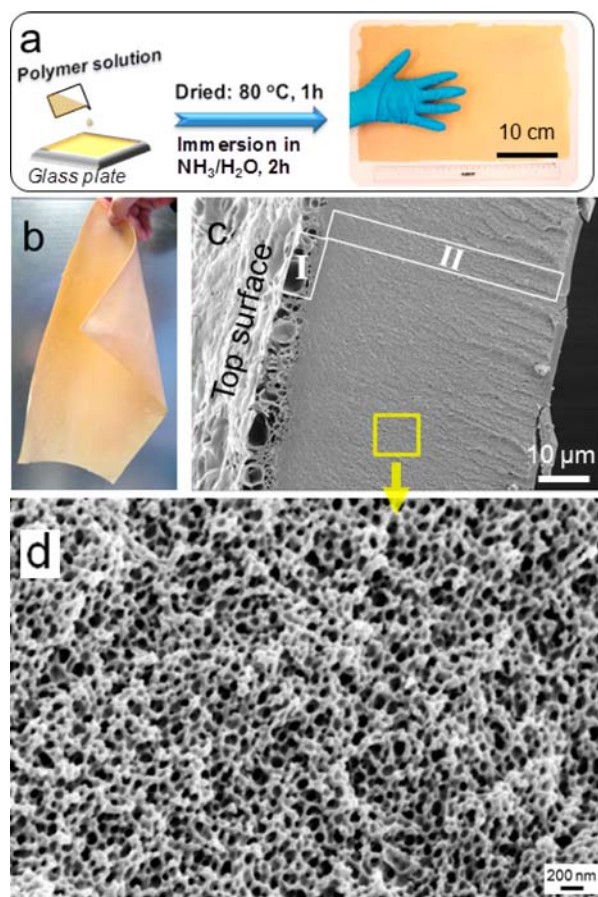


Figure 1. (a) Scheme for the preparation of a nanoporous polyelectrolyte membrane (PPM) from a solution mixture of a cationic poly(ionic liquid) and poly(acrylic acid) in DMF. (b) Photograph of a 35 cm \times 25 cm free-standing PPM. (c, d) Representative SEM images of the cross-sectional area of the as-prepared PPM.

promotes the polyelectrolyte membrane formation. Aqueous NH_3 solution in contact with the film surface diffuses into the polymer matrix, deprotonating the carboxylic acid (COOH)

groups of the PAA chains to form carboxylate groups (COO^-) and NH_4^+ ions. This triggers in situ ionic complexation of PAA with the surrounding PCMVImTf₂N chains to build up the electrostatically cross-linked network membrane. Fourier transform IR spectroscopy [Figure S2 in the Supporting Information (SI)] confirmed the presence of deprotonated carboxylate groups and the concomitant ionic complexation in the membrane. Because of the ionic bonding, the PCMVImTf₂N–PAA complex membrane is stable in water and all organic solvents, which is well-known behavior for most inter-polyelectrolyte complexes.^{7b} In contrast to the ionic complex, the PCMVImTf₂N/PAA blend without ionic bonding is soluble in DMF and dimethyl sulfoxide because of the lack of network formation.

Interestingly, a hierarchical nanopore structure was created simultaneously during the soaking step (Figure 1c,d). The vicinity of the top surface (zone I) is composed of micrometer/submicrometer-sized random pores. The layer underneath (zone II) is a three-dimensionally interconnected pore system with pore sizes between 30 and 100 nm (Figure 1d). Before NH_3 activation, the cross-section of the film was dense and pore-free (Figure S4). This proves that the pore formation is coupled to the structural rearrangements due to NH_3 -triggered interchain ionic bonding. We noticed that only a tiny fraction (<1 wt %) remained in the polymer blend system after the film drying step (Figure S5), excluding the possibility that the pore formation followed the NIPS mechanism, which is widely used by membrane industry to create sponge- or finger-type pores.^{1g} In fact, standard NIPS processing of the current PCMVImTf₂N/PAA mixture solution without the drying step produced only irregular precipitates without membrane cohesion.

From a kinetic point of view, the diffusion of aqueous NH_3 into the membrane matrix is the crucial step (Figure 2a). When the dried PCMVImTf₂N/PAA film is subsequently immersed in aqueous NH_3 solution, rapid and thorough electrostatic complexation takes place in the surface region because of the direct and full contact with the solution. After this stage, aqueous NH_3 gradually diffuses into the bulk membrane, coupling further interchain electrostatic complexation with pore-controlled mass transport. Driven by this intrinsically

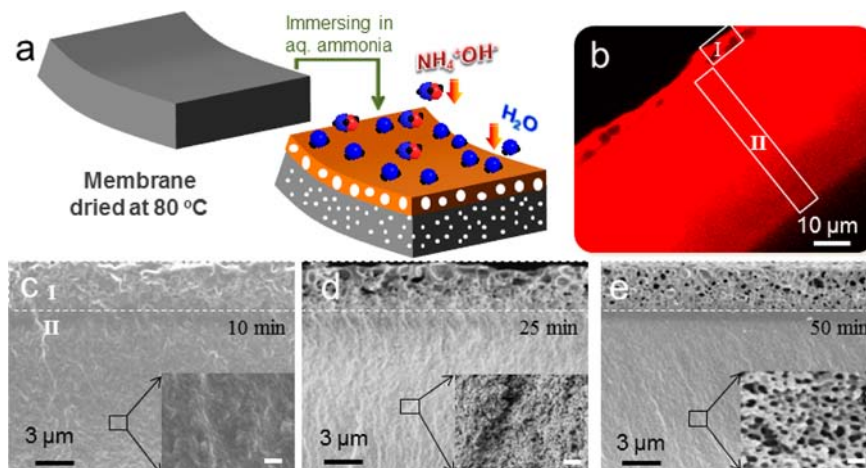


Figure 2. (a) Cartoon illustrating pore generation controlled by the diffusion of aqueous NH_3 into the membrane. (b) Fluorescent confocal laser scanning microscopy image of the PPM cross section after the film was soaked for 2 h in 0.2 wt % aqueous NH_3 doped with 15 ppm rhodamine B. (c–e) Time-dependent cross-section structures of the membrane soaked in 0.2 wt % aqueous NH_3 for 10, 25, and 50 min, respectively. Scale bars in the insets are 100 nm.

spontaneous ionic complexation process,^{7b} the polymer chains rearrange themselves in the polymer matrix to achieve a high degree of charge complexation, which is possible only in a nanoporous state. It is important to state that the film swells gradually with water, indicating that the pore structure is not due to a density increase but in fact is due to leftover pools of water.

Indeed, fluorescent confocal laser scanning microscopy was used to visualize the diffusion of rhodamine B-labeled aqueous NH_3 into the membrane cross section (Figure 2b). Time-dependent scanning electron microscopy (SEM) examination showed that large pores in zone I developed in the early stage of soaking, while at the same time zone II basically remained dense (Figure 2c,d). In later stages, zone I developed into its final macroporous morphology, while the nanopore system grew down into zone II with increasing soaking time (Figure 2e). Moreover, energy-dispersive X-ray analysis (Figure S6) confirmed that the degree of ionic complexation in zone I was larger than that in zone II. All of these results are supportive of a directional diffusion-controlled pore formation mechanism.

One might discuss why electrostatic complexation of other polyelectrolyte pairs reported in the literature has to date produced only dense, nanopore-free membranes.⁷ We believe that the PCMVImTf₂N/PAA system described here differs from previous ones in terms of the water insolubility of PCMVImTf₂N caused by its large hydrophobic Tf₂N⁻ counteranion. In this model, PCMVImTf₂N acts as a stable barrier against direct water swelling, avoiding “meltdown” or excessive swelling of the membrane matrix before the ionic network is fully developed; that is, partial swelling and ionic complexation go hand-in-hand throughout the soaking procedure. This is crucial for the dynamic pore formation process. Straightforward proof of this explanation can be obtained from Figure S7, wherein the PIL water solubility was varied by varying the counteranion from Br⁻ to BF₄⁻ to PF₆⁻. These anions follow the hydrophilicity sequence order Br⁻ >> BF₄⁻ ≈ PF₆⁻ > Tf₂N⁻.^{8c} As expected, no membrane could be formed from the PCMVImBr/PAA system because both polymer components are water-soluble. The PILs with BF₄⁻ and PF₆⁻ are water-insoluble. Consequently, porous membranes with similar hierarchical pore architectures but larger pore sizes were produced. Therefore, it seems that the hydrophobicity of the PIL is an indispensable prerequisite for the development of nanoporous membranes. This rule was even successfully expanded to other cationic polyelectrolytes (Figure S8).

The integration of hierarchically structured pores and electrostatic charge into the current PPM network indeed creates a multifunctional platform that is appealing for separation, catalysis, and many more applications. In addition, the PPM coating procedure is highly applicable for device fabrication because the PIL components are surface-active materials.⁹ This means that very homogeneous and also defect-free coatings are formed even on nonplanar or complex curved objects, as the film homogeneity is driven by interface and spreading effects. Currently, fiber-optic sensors are particularly valued for their miniaturized sizes that allow access to confined micrometer environments, their stability against electromagnetic interference or harsh conditions, and their capability for remote online monitoring.¹⁰ They are becoming increasingly important in chemical analysis of the environment, production monitoring, molecular biotechnology, the automotive industry, and so on.^{10b} In a typical sensing experiment, the

sensitivity of the transmission spectrum of an optical-fiber sensor to variations of its external refractive index is used. Accordingly, polyelectrolytes have often been assembled onto optical fibers to prepare pH sensors because their degree of swelling and refractive index are responsive to environmental pH.^{8e,11} The drawback of common polymer-coated fiber-optic sensors is that their coatings are either unfavorably dense or thin, making the sensing process either sluggish or less sensitive.

As an example of a potential application, the PCMVImTf₂N/PAA nanoporous membrane was coated onto a thin-core fiber interferometer (TCFMI) with a diameter of 125 μm via the processing scheme shown in Figure 1a (see Figure S9). The performance of the freshly prepared fiber-optic sensor was tested as the pH was increased from 2 to 10 and then decreased from 10 back to 2. Indeed, a fairly reproducible wavelength–pH correlation was observed in both runs (Figure 3a). The

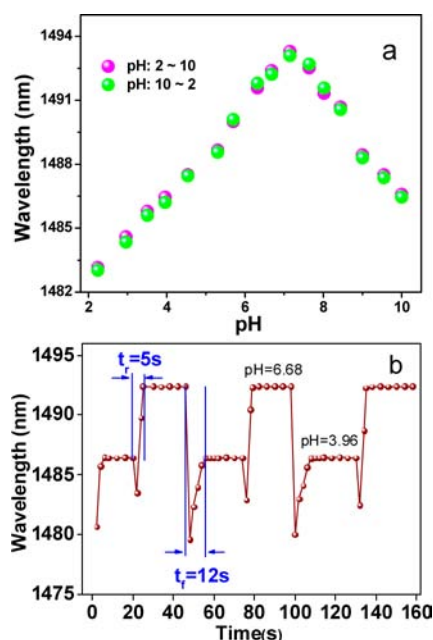


Figure 3. (a) Response of the TCFMI pH sensor versus pH. The original spectra are shown in Figure S10. (b) Dynamic responses of the TCFMI pH sensor in solutions with pH alternating between 6.68 and 3.96.

transmitted wavelength of the TCFMI sensor first increased and then decreased linearly with pH before and after a turning point at pH 7. This nonmonotonic change in the wavelength as a function of pH is well-known in sensing devices prepared from LbL coatings because the electrostatic complexation is the strongest at neutral pH.^{8c} Consequently, the coating is least swollen^{8e,12} at this point and reaches the highest refractive index. In addition to the reversibility, the sensitivity of the prepared TCFMI pH sensor was particularly high [2.04 and -2.48 nm/pH unit in the acidic (pH 2–7) and alkaline (pH 7–10) regions, respectively; see Table S1 in the SI]. Remarkably, such high sensitivity was coupled to a fast response time. For example, a stable signal was observed within only 5 s (t_r) after the pH was varied from 3.96 to 6.68 and within 12 s (t_f) after the pH returned from 6.68 to 3.96 (Figure 3b). This response is much faster than those of other types of polymer-coated fiber-optic sensors, which usually require tens to hundreds of seconds. Traditionally, an improvement in sensitivity usually

sacrifices the response rate and vice versa. It is obvious that the current nanoporous PPM coating gives a high sensitivity with a simultaneously enhanced response rate, which is due to the optimized liquid transport within the film. This makes the current sensor exceptional and superior to the common LbL coating setups (Table S1).^{8e,13} As a reference experiment, we also constructed a control TCFMI pH sensor with the nonporous PCMVImTf₂N/PAA blend film, which showed much longer response times ($t_r = 45$ s and $t_f = 120$ s; see Figure S11).

In summary, we have introduced a template-free and scalable method to prepare hierarchically structured nanoporous polyelectrolyte membranes using a simple film-casting and solution immersion/activation procedure. Both membrane and pore formation are promoted simultaneously by the NH₃-triggered in situ ionic complexation between a hydrophobic PIL and deprotonated poly(acrylic acid). The membranes, which consist of a thin layer of surface macropores followed by a thick layer of three-dimensionally interconnected nanopores (30–100 nm), are robust and stable in water and common organic solvents. Being simultaneously charged and nanoporous in nature, these membranes are highly promising for a broad range of applications. An optical fiber coated with such a membrane was demonstrated to break the common “trade-off” rule in sensor applications, showing superior pH sensing performance with a fast response ($t_r = 5$ s, $t_f = 12$ s) and high sensitivity (2.04 and -2.48 nm/pH unit). Since solution casting is an industrially well-established membrane formation procedure and the PILs are surface-active materials with a multitude of functionalities, the method developed in this study paves a much broader way for the preparation of nanoporous polyelectrolyte films and coatings.

■ ASSOCIATED CONTENT

Supporting Information

Materials and membrane characterizations. This material is available free of charge via the Internet at <http://pubs.acs.org>.

■ AUTHOR INFORMATION

Corresponding Author

jiayin.yuan@mpikg.mpg.de

Notes

The authors declare no competing financial interest.

■ ACKNOWLEDGMENTS

The authors thank the Max Planck Society for financial support. Q.Z. acknowledges a Lindau Fellowship (GZ 725) provided by the Sino-German Center. The authors thank Dr. H. Q. Wang for fluorescent confocal laser scanning microscopy measurements, Dr. Christoph Wieland for gel-permeation chromatography measurements, and Prof. Litang Yan for helpful discussions.

■ REFERENCES

(1) (a) Wu, D.; Xu, F.; Sun, B.; Fu, R.; He, H.; Matyjaszewski, K. *Chem. Rev.* **2012**, *112*, 3959. (b) Shannon, M. A.; Bohn, P. W.; Elimelech, M.; Georgiadis, J. G.; Marinas, B. J.; Mayes, A. M. *Nature* **2008**, *452*, 301. (c) Gin, D. L.; Noble, R. D. *Science* **2011**, *332*, 674. (d) Dawson, R.; Cooper, A. I.; Adams, D. J. *Prog. Polym. Sci.* **2012**, *37*, 530. (e) Ulbricht, M. *Polymer* **2006**, *47*, 2217. (f) Hernandez-Guerrero, M.; Stenzel, M. H. *Polym. Chem.* **2012**, *3*, 563. (g) Peinemann, K. V.; Abetz, V.; Simon, P. F. W. *Nat. Mater.* **2007**,

6, 992. (h) Wan, L. S.; Li, J. W.; Ke, B. B.; Xu, Z. K. *J. Am. Chem. Soc.* **2012**, *134*, 95.

(2) (a) Ballauff, M. *Prog. Polym. Sci.* **2007**, *32*, 1135. (b) Dotzauer, D. M.; Dai, J.; Sun, L.; Bruening, M. L. *Nano Lett.* **2006**, *6*, 2268. (c) Hu, X.; Huang, J.; Zhang, W.; Li, M.; Tao, C.; Li, G. *Adv. Mater.* **2008**, *20*, 4074. (d) Tokarev, I.; Orlov, M.; Minko, S. *Adv. Mater.* **2006**, *18*, 2458. (e) Rahmthullah, M. A. M.; Snyder, J. D.; Elabd, Y. A.; Palmese, G. R. *J. Polym. Sci., Part B: Polym. Phys.* **2010**, *48*, 1245.

(3) (a) Pitet, L. M.; Amendt, M. A.; Hillmyer, M. A. *J. Am. Chem. Soc.* **2010**, *132*, 8230. (b) Le, L.; Xiaobo, S.; Sung Woo, H.; Hayward, R. C.; Russell, T. P. *Angew. Chem., Int. Ed.* **2012**, *51*, 4089. (c) Zhao, H.; Gu, W.; Sterner, E.; Russell, T. P.; Coughlin, E. B.; Theato, P. *Macromolecules* **2011**, *44*, 6433. (d) Xue, L.; Zhang, J.; Han, Y. *Prog. Polym. Sci.* **2012**, *37*, 564.

(4) (a) Hariri, H. H.; Schlenoff, J. B. *Macromolecules* **2010**, *43*, 8656. (b) Mjahed, H.; Porcel, C.; Senger, B.; Chassepot, A.; Netter, P.; Gillet, P.; Decher, G.; Voegel, J. C.; Schaaf, P.; Benkirane Jessel, N.; Boulmedais, F. *Soft Matter* **2008**, *4*, 1422. (c) Gopishetty, V.; Roiter, Y.; Tokarev, I.; Minko, S. *Adv. Mater.* **2008**, *20*, 4588. (d) Chen, J.; Xia, X. M.; Huang, S. W.; Zhuo, R. X. *Adv. Mater.* **2007**, *19*, 979. (e) Zhang, L.; Zheng, M.; Liu, X.; Sun, J. *Langmuir* **2011**, *27*, 1346.

(5) (a) Hiller, J.; Mendelsohn, J. D.; Rubner, M. F. *Nat. Mater.* **2002**, *1*, 59. (b) Mendelsohn, J. D.; Barrett, C. J.; Chan, V. V.; Pal, A. J.; Mayes, A. M.; Rubner, M. F. *Langmuir* **2000**, *16*, 5017. (c) Lutkenhaus, J. L.; McEnnis, K.; Hammond, P. T. *Macromolecules* **2008**, *41*, 6047. (d) Lowman, G. M.; Tokuhisa, H.; Lutkenhaus, J. L.; Hammond, P. T. *Langmuir* **2004**, *20*, 9791. (e) Cho, J.; Hong, J.; Char, K.; Caruso, F. *J. Am. Chem. Soc.* **2006**, *128*, 9935. (f) Li, Q.; Quinn, J. F.; Caruso, F. *Adv. Mater.* **2005**, *17*, 2058. (g) Zimmitsky, D.; Shevchenko, V. V.; Tsukruk, V. V. *Langmuir* **2008**, *24*, 5996.

(6) (a) Decher, G. *Science* **1997**, *277*, 1232. (b) Decher, G.; Schlenoff, J. B. *Multilayer Thin Films: Sequential Assembly of Nanocomposite Materials*, 2nd ed.; Wiley-VCH: Weinheim, Germany, 2012.

(7) (a) Zhao, Q.; An, Q. F.; Ji, Y.; Qian, J.; Gao, C. *J. Membr. Sci.* **2011**, *379*, 19. (b) Thünemann, A. F.; Müller, M.; Dautzenberg, H.; Joanny, J. F.; Löwen, H. *Adv. Polym. Sci.* **2004**, *166*, 113. (c) Sukhishvili, S. A.; Kharlampieva, E.; Izumrudov, V. *Macromolecules* **2006**, *39*, 8873. (d) Pergushov, D. V.; Müller, A. H. E.; Schacher, F. H. *Chem. Soc. Rev.* **2012**, *41*, 6888.

(8) (a) Lu, J.; Yan, F.; Texter, J. *Prog. Polym. Sci.* **2009**, *34*, 431. (b) Mecerreyes, D. *Prog. Polym. Sci.* **2011**, *36*, 1629. (c) Yuan, J.; Antonietti, M. *Polymer* **2011**, *52*, 1469. (d) Green, O.; Grubjesic, S.; Lee, S.; Firestone, M. A. *Polym. Rev.* **2009**, *49*, 339. (e) Yuan, J.; Soll, S.; Drechsler, M.; Müller, A. H. E.; Antonietti, M. *J. Am. Chem. Soc.* **2011**, *133*, 17556. (f) Zhao, Q.; Zhang, P.; Antonietti, M.; Yuan, J. *J. Am. Chem. Soc.* **2012**, *134*, 11852. (g) Sui, X.; Hempenius, M. A.; Vancso, G. J. *J. Am. Chem. Soc.* **2012**, *134*, 4023. (h) Tang, J.; Radosz, M.; Shen, Y. *Macromolecules* **2008**, *41*, 493. (i) Green, M. D.; Long, T. E. *Polym. Rev.* **2009**, *49*, 291. (j) Ye, Y.; Choi, J.-H.; Winey, K. I.; Elabd, Y. A. *Macromolecules* **2012**, *45*, 7027.

(9) Texter, J. *Macromol. Rapid Commun.* **2012**, *33*, 1996.

(10) (a) Flusberg, B. A.; Cocker, E. D.; Piyawattanametha, W.; Jung, J. C.; Cheung, E. L. M.; Schnitzer, M. J. *Nat. Methods* **2005**, *2*, 941. (b) Wang, X. D.; Wolfbeis, O. S. *Anal. Chem.* **2013**, *85*, 487. (c) Ma, C.; Wang, A. *Appl. Opt.* **2013**, *52*, 127. (d) Wang, D. Y.; Wang, Y.; Gong, J.; Wang, A. *Opt. Lett.* **2011**, *36*, 3392. (e) Lindner, E.; Canning, J.; Chojetzki, C.; Brückner, S.; Becker, M.; Rothhardt, M.; Bartelt, H. *Opt. Commun.* **2011**, *284*, 183. (f) Jewart, C. M.; Wang, Q.; Canning, J.; Grobnc, D.; Mihailov, S. J.; Chen, K. P. *Opt. Lett.* **2010**, *35*, 1443.

(11) Gu, B.; Yin, M. J.; Zhang, A. P.; Qian, J. W.; He, S. *Opt. Express* **2009**, *17*, 22296.

(12) (a) Burke, S. E.; Barrett, C. J. *Macromolecules* **2004**, *37*, 5375. (b) Annaka, M.; Tanaka, T. *Nature* **1992**, *355*, 430.

(13) Gu, B.; Yin, M.; Zhang, A. P.; Qian, J.; He, S. *IEEE Sens. J.* **2012**, *12*, 1477.